

Communication-Efficient Stochastic Zeroth-Order Optimization for Federated Learning

Wenzhi Fang, Ziyi Yu, Yuning Jiang, Yuanming Shi, Colin N. Jones, and Yong Zhou

Abstract—Federated learning (FL), as an emerging edge artificial intelligence paradigm, enables many edge devices to collaboratively train a global model without sharing their private data. To enhance the training efficiency of FL, various algorithms have been proposed, ranging from first-order to second-order methods. However, these algorithms cannot be applied in scenarios where the gradient information is not available, e.g., federated black-box attack and federated hyperparameter tuning. To address this issue, in this paper we propose a derivative-free federated zeroth-order optimization (FedZO) algorithm featured by performing multiple local updates based on stochastic gradient estimators in each communication round and enabling partial device participation. Under the non-convex setting, we derive the convergence performance of the FedZO algorithm and characterize the impact of the numbers of local iterates and participating edge devices on the convergence. To enable communication-efficient FedZO over wireless networks, we further propose an over-the-air computation (AirComp) assisted FedZO algorithm. With an appropriate transceiver design, we show that the convergence of AirComp-assisted FedZO can still be preserved under certain signal-to-noise ratio conditions. Simulation results demonstrate the effectiveness of the FedZO algorithm and validate the theoretical observations.

Index Terms—Federated learning, zeroth-order optimization, convergence, over-the-air computation.

I. INTRODUCTION

With the rapid advancement of the Internet of Things (IoT), a massive amount of data is generated and collected by various edge devices (e.g., sensors, smart phones). Because of the limited radio spectrum resource and increasing privacy concerns, gathering geographically distributed data from a large number of edge devices into a cloud server to enable cloud artificial intelligence (AI) may not be practical. To this end, edge AI has recently been envisioned as a promising AI paradigm [1]. Unlike cloud AI that relies on a cloud server to conduct centralized training, edge AI exploits the computing power of multiple edge devices to perform model training with their own local data in a distributed manner. Federated learning (FL) [2], as a representative edge AI framework, enables multiple edge devices to collaboratively train a shared model without exchanging their local data, which effectively alleviates the communication burden and privacy concerns. Nowadays, FL has found application in various fields, including autonomous driving [3], recommendation systems [4], healthcare informatics [5], etc.

Wenzhi Fang, Ziyi Yu, Yuanming Shi, and Yong Zhou are with the School of Information Science and Technology, ShanghaiTech University, Shanghai 201210, China (e-mail: {fangwzh1, yuzy, shiym, zhouyong}@shanghaitech.edu.cn).

Yuning Jiang and Colin N. Jones are with Automatic Control Laboratory, EPFL, Switzerland (e-mail: {yunying.jiang, colin.jones}@epfl.ch).

As a result of the popularity of FL, the federated optimization problem for model training has attracted a growing body of attention from both academia and industry in recent years. Various algorithms have been proposed to attain a fast convergence rate and reduce the communication load, including both first- (e.g., FedAvg [2], FedPD [6], FedNova [7]) and second-order algorithms (e.g., FedDANE [8]). Most existing algorithms rely on gradient and/or Hessian information to solve the federated optimization problem. However, such information cannot be obtained in scenarios where the analytic expressions of the loss functions are unavailable, such as for federated hyperparameter tuning [9] or distributed black-box attack of deep neural networks (DNN) [10]. In other words, existing algorithms cannot tackle federated optimization problems when gradient information is not available. This motivates us to develop a communication-efficient federated zeroth-order optimization algorithm that does not require gradient or Hessian information.

Parallel with the research on algorithm design for FL, the implementation of FL over wireless networks is also an emerging research topic. Random channel fading and receiver noise raise unique challenges for the training of FL over wireless networks. Guaranteeing the learning performance with limited radio resource is a challenging task, which requires the joint design of the learning algorithm and communication strategy. Along this line of research, the authors in [11], [12] studied the joint resource allocation and edge device selection to enhance learning performance. Both studies adopted the orthogonal multiple access (OMA) scheme, where the number of edge devices that can participate in each communication round is restricted by the number of available time/frequency resource blocks. The limited radio resource turns out to be the main performance bottleneck of wireless FL. Fortunately, over-the-air computation (AirComp), as a non-orthogonal multiple access scheme, allows concurrent transmissions over the same radio channel to enable low-latency and spectrum-efficient wireless data aggregation [13]–[15], thereby mitigating the communication bottleneck [16]. Motivated by this observation, various AirComp-assisted FL algorithms were proposed in [17]–[19] to achieve fast model aggregation, wherein all of them adopted first-order optimization algorithm. There still lacks a thorough investigation on AirComp-assisted FL with zeroth-order optimization.

A. Main Contributions

In this paper, we consider a federated optimization problem, where the gradient of the loss function is not available. We

propose a derivative-free federated zeroth-order optimization algorithm, named FedZO, whose key feature is performing multiple local updates based on a two-point stochastic gradient estimator in each communication round and enabling partial device participation. We establish a convergence guarantee for the proposed FedZO algorithm and study its implementation over wireless networks with the assistance of AirComp, which is challenging for the following reasons. First, although executing multiple local iterates in each communication round reduces the communication overhead, it also increases the discrepancies among local models due to the data heterogeneity and may even lead to algorithmic divergence. To reduce the communication overhead while preserving the convergence, the relationship between the convergence behavior and the number of local iterates needs to be characterized. Second, the stochastic gradient estimator adopted in FedZO is not an unbiased estimate of the actual gradient, and the variance of the stochastic gradient estimator may not be bounded. These unique features together with multiple local iterates and partial device participation per communication round make the existing convergence analysis framework for FedAvg not applicable to the proposed FedZO algorithm. Third, to characterize the convergence of the AirComp-assisted FedZO algorithm, the impact of the random channel fading and receiver noise in global model aggregation needs to be further taken into account. This not only complicates the convergence analysis but also poses a new problem for the communication strategy design. In this paper, we develop a unified convergence analysis framework to address the aforementioned challenges. The main contributions of this paper are summarized as follows:

- We develop the derivative-free FedZO algorithm, which inherits the framework of the FedAvg algorithm but only queries the values of the objective function, to handle federated optimization problems without using gradient and Hessian information. To cater for the FL system with a large number of edge devices and to reduce the communication overhead, the proposed FedZO algorithm enables partial device participation and performs multiple local iterates in each communication round.
- We establish a convergence guarantee for the proposed FedZO algorithm in a non-convex setting and derive the maximum number of local iterates required for preserving convergence. We demonstrate that the proposed FedZO algorithm can attain linear speedup in the number of the local iterates and the number of participating edge devices.
- We study the implementation of the FedZO algorithm over wireless networks with the assistance of AirComp for the aggregation of local model updates in the uplink. With an appropriate transceiver design that can mitigate the impact of the fading and noise perturbation, we study the convergence behavior of the AirComp-assisted FedZO algorithm and characterize the impact of the signal-to-noise ratio (SNR) on the convergence rate.

We conduct extensive simulations to evaluate the performance of the proposed FedZO and AirComp-assisted FedZO algorithms. Simulation results show that the proposed FedZO

algorithm is convergent under various parameter settings and outperforms existing distributed zeroth-order method. Moreover, simulations illustrate that the performance of the proposed FedZO algorithm is comparable to that of the FedAvg algorithm, which indicates that the proposed FedZO algorithm can serve as a satisfactory alternative for FedAvg when first-order information is not available. Results also confirm that, with an appropriate SNR setting, the AirComp-assisted FedZO algorithm preserves convergence.

B. Related Works

The study of FL started from the seminal work [2], where the authors proposed a communication-efficient federated optimization algorithm known as FedAvg. Subsequently, various articles established convergence guarantees for the FedAvg algorithm [20]–[22]. Following the FedAvg algorithm, many other first-order methods have been proposed, e.g., FedNova [7], FedProx [23], SCAFFOLD [24], FedSplit [25], and FedPD [6]. To further reduce the communication overhead, several second-order optimization algorithms were proposed, such as GIANT [26] and FedDANE [8]. Although the aforementioned first- and second-order algorithms have broad applications, there are still many FL tasks where the gradient and Hessian information are unavailable and thus require zeroth-order optimization.

Recently, several works [10], [27]–[29] focused on studying distributed zeroth-order optimization. Specifically, the authors in [27] developed a so-called ZONE algorithm based on the primal-dual technique. In [28], the authors employed the gradient tracking technique to develop a distributed zeroth-order algorithm, which attains convergence rate $\mathcal{O}\left(\frac{d}{T}\right)$, where T and d denote the number of total iterates and the dimension of model parameters, respectively. However, ZONE requires $\mathcal{O}(T)$ sampling complexity per iteration while the algorithm proposed in [28] considered the deterministic setting. The authors in [10] concentrated on the stochastic setup and proposed an algorithm with convergence rate $\mathcal{O}\left(\sqrt{d/(NT)}\right)$ and sampling complexity $\mathcal{O}(1)$, where N denotes the number of edge devices. More recently, the authors in [29] proposed a decentralized zeroth-order algorithm that allows multiple local updates. However, the theoretic analysis in [29] focused on the strongly convex scenario and relied on the bounded gradient assumption, which are relatively restrictive [30]. Moreover, most of the existing distributed zeroth-order algorithms focused on full device participation, which may not be practical for FL systems with limited radio resource and a large number of edge devices [21].

AirComp has recently been adopted to support the implementation of FL over wireless networks [17], [31]–[35], where channel fading and receiver noise inevitably distort the model aggregation, and in turn introduce a detrimental impact on the learning performance [17]. The convergence behavior of various FL algorithms, e.g., vanilla gradient method [31] and stochastic gradient method [32], showed that the channel fading and noise perturbation typically introduce a non-diminishing optimality gap, which can be mitigated by transmit power control [32], beamforming design [31], and device

scheduling [33]. In [34], the authors proposed a joint learning and transmission scheme to ensure global convergence for strongly convex problems. By utilizing the communication strategy in [34], the authors in [35] developed an AirComp-assisted accelerated gradient descent algorithm. Despite the above progress, the existing works focused on the first-order method, while there is no relevant literature studying the AirComp-assisted zeroth-order optimization algorithm.

C. Organization

The remainder of this paper is organized as follows. We present the problem formulation and propose a federated zeroth-order optimization algorithm in Section II. Section III provides the convergence analysis. Section IV studies the implementation of the proposed FedZO algorithm over wireless networks using AirComp. The simulation results are provided in Section V. Finally, we conclude this paper in Section VI.

II. FEDERATED ZERO-ORDER OPTIMIZATION

In this section, we first introduce the federated optimization problem and then propose a federated zeroth-order optimization algorithm.

A. Problem Formulation

Consider an FL task over a network consisting of a central server and N edge devices indexed by $\{1, 2, \dots, N\}$. The goal of the central server is to coordinate all edge devices to collaboratively solve the following federated optimization problem

$$\min_{\mathbf{x} \in \mathbb{R}^d} f(\mathbf{x}) \triangleq \frac{1}{N} \sum_{i=1}^N f_i(\mathbf{x}), \quad (1)$$

where $\mathbf{x} \in \mathbb{R}^d$ denotes the model parameter of dimension d , and $f_i(\mathbf{x})$ and $f(\mathbf{x})$ denote the local loss function of edge device i and the global loss function at the central server evaluated at model parameter \mathbf{x} , respectively. We assume that each edge device with a local dataset is equally important for the global model [22]. In (1), $f_i(\mathbf{x})$ measures the expected risk over the local data distribution denoted as \mathcal{D}_i at edge device i , given by

$$f_i(\mathbf{x}) \triangleq \mathbb{E}_{\xi_i \sim \mathcal{D}_i} [F_i(\mathbf{x}, \xi_i)],$$

where $\xi_i \sim \mathcal{D}_i$ represents a random variable ξ_i uniformly sampled from \mathcal{D}_i , and $F_i(\mathbf{x}, \xi_i)$ represents the loss with respect to ξ_i evaluated at model parameter \mathbf{x} .

The FedAvg algorithm [2], as a popular gradient-based method, can be applied to tackle the federated optimization problem (1). In particular, each edge device performs multiple steps of stochastic gradient descent with respect to its local loss function at each round. The resulting model updates of all edge devices are transmitted to the central server and then averaged to obtain an updated global model for the next round. However, the FedAvg algorithm is gradient-based, and cannot be applied to scenarios where gradient information is not available. Such scenarios arise in many practical applications, including but not limited to federated black-box attacks of DNN [10] and federated hyperparameter tuning in model training [9].

To be specific, in federated black-box attacks, the gradient information cannot be acquired as the deep model is hidden. In the federated hyperparameter tuning task, there does not exist an analytic relationship between the training loss and the hyperparameters. Besides, the FedAvg algorithm may not be efficient in the scenario where the calculation of the gradient is expensive, such as for online sensor selection scenario in which the gradient computation involves a matrix inverse operation [36]. Motivated by these observations, this paper focuses on solving problem (1) via a zeroth-order optimization method by only querying the values of the objective function, i.e., without using gradient information.

B. FedZO Algorithm

Inspired by the FedAvg algorithm, we develop a federated zeroth-order optimization algorithm summarized in Algorithm 1. The main idea of the FedZO algorithm is to get rid of the dependence on the gradient and reduce the frequency of model exchanges, which are achieved by employing a gradient estimator and performing H steps of stochastic zeroth-order updates per communication round, respectively. The FedZO algorithm consists of the following four phases in each round.

- *Global Model Dissemination:* At the beginning of the t -th round, the central server uniformly samples M edge devices to participate in the local training. The set of scheduled edge devices in round t is denoted as \mathcal{M}_t . Then, the central server disseminates its current global model parameter \mathbf{x}^t to the selected edge devices.
- *Local Model Update:* After receiving the model parameter \mathbf{x}^t from the central server, each edge device $i \in \mathcal{M}_t$ initializes its local model $\mathbf{x}_i^{(t,0)}$ with the received global model from the central server, i.e., $\mathbf{x}_i^{(t,0)} = \mathbf{x}^t$, and then takes a total of H iterates of stochastic zeroth-order updates. In particular, at the k -th iterate of the t -th round, edge device i computes a two-point stochastic gradient estimator [28] as follows

$$\begin{aligned} & \tilde{\nabla}_v^\mu F_i(\mathbf{x}_i^{(t,k)}, \xi_i^{(t,k)}) \\ &= \frac{d\mathbf{v}^{(t,k)}}{\mu_t} \left(F_i(\mathbf{x}_i^{(t,k)} + \mu_t \mathbf{v}^{(t,k)}, \xi_i^{(t,k)}) - F_i(\mathbf{x}_i^{(t,k)}, \xi_i^{(t,k)}) \right), \end{aligned} \quad (2)$$

where $\mathbf{x}_i^{(t,k)}$ and $\xi_i^{(t,k)}$ represent the local model of edge device i and a random variable sampled by edge device i based on its local data distribution \mathcal{D}_i at the k -th iterate of the t -th round, respectively. $\mathbf{v}^{(t,k)}$ is a d -dimensional random direction that is uniformly sampled from a unit sphere \mathbb{S}^d , and μ_t is a positive step size. Subsequently, the sampled edge devices update their local models by performing the following stochastic zeroth-order update

$$\mathbf{x}_i^{(t,k+1)} = \mathbf{x}_i^{(t,k)} - \eta_t \tilde{\nabla}_v^\mu F_i(\mathbf{x}_i^{(t,k)}, \xi_i^{(t,k)}), \quad k = 0, 1, \dots, H-1,$$

where η_t denotes the learning rate. After H local iterates, edge device i obtains an updated local model $\mathbf{x}_i^{(t,H)}$.

- *Local Model Uploading:* All edge devices in set \mathcal{M}_t calculate the updates of their local models in this round, i.e., $\Delta_i^t = \mathbf{x}_i^{(t,H)} - \mathbf{x}_i^{(t,0)}$, $i \in \mathcal{M}_t$, and then upload these updates to the central server.

Algorithm 1: FedZO Algorithm

Input: Initial model \mathbf{x}^0 , learning rate η_t , step size μ_t , number of participating edge devices M

for $t \in \{0, 1, \dots, T-1\}$ **do**

Uniformly sample a subset \mathcal{M}_t of M edge devices

Disseminate global model \mathbf{x}^t to all edge devices in set \mathcal{M}_t

for edge device $i \in \mathcal{M}_t$ **in parallel do**

Initialize local model $\mathbf{x}_i^{(t,0)} = \mathbf{x}^t$

for $k = 0, \dots, H-1$ **do**

Compute local stochastic gradient estimator $\tilde{\nabla}_v^\mu F_i(\mathbf{x}_i^{(t,k)}, \xi_i^{(t,k)})$ according to (2)

Perform local update $\mathbf{x}_i^{(t,k+1)} = \mathbf{x}_i^{(t,k)} - \eta_t \tilde{\nabla}_v^\mu F_i(\mathbf{x}_i^{(t,k)}, \xi_i^{(t,k)})$

end

Compute local model updates $\Delta_i^t = \mathbf{x}_i^{(t,H)} - \mathbf{x}_i^{(t,0)}$

Upload local model updates to central server

end

Aggregate local changes $\Delta^t = \frac{1}{M} \sum_{i \in \mathcal{M}_t} \Delta_i^t$

Update global model $\mathbf{x}^{t+1} = \mathbf{x}^t + \Delta^t$

end

- *Global Model Update:* After receiving local model updates from the sampled edge devices, the central server aggregates these updates, i.e., $\Delta^t = \frac{1}{M} \sum_{i \in \mathcal{M}_t} \Delta_i^t$, and then updates the global model, i.e., $\mathbf{x}^{t+1} = \mathbf{x}^t + \Delta^t$.

Although the proposed FedZO algorithm adopts a similar framework as the FedAvg algorithm, the convergence analysis of the latter cannot be directly extended to that of the FedZO algorithm. The key factor hindering the extension is that the gradient estimator does not preserve specific properties of the stochastic gradient. For instance, the gradient estimator (2) is not an unbiased estimate of the true gradient. Moreover, the variance of the gradient estimator may not be bounded. However, the stochastic gradient with a bounded variance is a basic assumption in existing stochastic first-order optimization algorithms [6], [7]. Besides, the existing theoretical analysis framework for the distributed zeroth-order optimization method cannot be applied to the FedZO algorithm as existing zeroth-order algorithms [10], [27], [28] do not consider multiple steps of local model updates and partial device participation. A larger number of local iterates reduces the communication overhead, but also increases the local model discrepancies and may even lead to algorithmic divergence. To preserve convergence for the developed FedZO algorithm, it is necessary to bound these discrepancies by appropriately choosing the number of local updates, i.e., H . In Section III, we will provide the convergence analysis for the FedZO algorithm.

III. CONVERGENCE ANALYSIS FOR FEDZO

In this section, we present the convergence analysis of the FedZO algorithm with full and partial device participation. To make our analysis applicable for more practical scenarios, we

focus on the setting of non-convex loss functions. We make the following assumptions for the tractability of convergence analysis.

Assumption 1. The global loss in (1), i.e., $f(\mathbf{x})$, is lower bounded by f_* , i.e., $f(\mathbf{x}) \geq f_* > -\infty$.

Assumption 2. We assume that all $F_i(\mathbf{x}, \xi_i)$, $f_i(\mathbf{x})$, and $f(\mathbf{x})$ are L -smooth. Mathematically, for any $\mathbf{x} \in \mathbb{R}^d$ and $\mathbf{y} \in \mathbb{R}^d$, we have

$$\begin{aligned} \|\nabla f_i(\mathbf{y}) - \nabla f_i(\mathbf{x})\| &\leq L\|\mathbf{y} - \mathbf{x}\|, \quad \forall i, \\ f(\mathbf{y}) &\leq f(\mathbf{x}) + \langle \nabla f(\mathbf{x}), \mathbf{y} - \mathbf{x} \rangle + \frac{L}{2} \|\mathbf{y} - \mathbf{x}\|^2, \end{aligned}$$

where $\|\cdot\|$ denotes the ℓ_2 norm.

Assumption 3. The stochastic gradient $\nabla F_i(\mathbf{x}, \xi_i)$ is an unbiased estimate of $\nabla f_i(\mathbf{x})$, i.e., $\mathbb{E}_{\xi_i}[\nabla F_i(\mathbf{x}, \xi_i)] = \nabla f_i(\mathbf{x})$, $\forall \mathbf{x} \in \mathbb{R}^d$, $\forall i$.

Assumption 4. The stochastic gradient has a bounded variance, i.e., there exists a constant σ_g such that $\mathbb{E}_{\xi_i} \|\nabla F_i(\mathbf{x}, \xi_i) - \nabla f_i(\mathbf{x})\|^2 \leq \sigma_g^2$, $\forall \mathbf{x} \in \mathbb{R}^d$, $\forall i$.

Assumption 5. The dissimilarity between each local loss function and the global loss function is bounded by σ_h^2 , i.e., $\|\nabla f(\mathbf{x}) - \nabla f_i(\mathbf{x})\|^2 \leq \sigma_h^2$, $\forall \mathbf{x} \in \mathbb{R}^d$, $\forall i$.

Assumptions 1-4 are commonly used in stochastic optimization [37]. Assumption 5 is extensively adopted in federated optimization to characterize the heterogeneity between the local and global losses [6], [22], and also considered in distributed zeroth-order optimization [10]. Note that these assumptions are only required for convergence analysis, as in [6], [10], [22]. In this section, we consider that learning rate η_t and step size μ_t are invariant during the training process, as in [7], [22], [30]. We thus omit their subscripts and denote them as η and μ .

In the following, we first present the convergence analysis for full device participation and then extend the analysis to partial device participation.

A. Full Device Participation

We first characterize the convergence of the FedZO algorithm with full device participation in Theorem 1. We take the squared gradient $\|\nabla f(\mathbf{x}^t)\|^2$ to evaluate the suboptimality of the iterates. The speed of approaching a stationary point is an important metric to evaluate the algorithmic effectiveness for non-convex problems [38].

Theorem 1. Suppose that Assumptions 1-5 hold and the learning rate satisfies

$$\eta \leq \min \left\{ \frac{N}{72dL}, \frac{2}{NH^2L}, \frac{1}{3\sqrt{dHL}} \right\}, \quad (3)$$

the FedZO algorithm with full device participation satisfies

$$\begin{aligned} \min_{t \in [T]} \mathbb{E} \|\nabla f(\mathbf{x}^t)\|^2 &\leq 4 \frac{f(\mathbf{x}^0) - f_*}{HT\eta} + \eta \frac{24dL}{N} (\sigma_g^2 + 3\sigma_h^2) \\ &\quad + \frac{dL^2\mu^2}{12} + 4L^2\mu^2, \end{aligned} \quad (4)$$

where $[T]$ denotes the index set of communication rounds, i.e., $[T] = \{0, 1, \dots, T-1\}$.

Proof. Please refer to Appendix A. \square

According to Theorem 1, the upper bound of the minimum squared gradient among the global model sequence is composed of four terms. The first term shows that the convergence rate relies on the initial sub-optimality. The second term shows that the convergence rate depends on the stochastic gradient variance and statistical heterogeneity. The rest of the terms are related to step size μ for computing the gradient estimator that is unique in zeroth-order optimization. As pointed out in [38], we can select an appropriate step size to attain the desired accuracy. The following corollary follows by substituting a suitable learning rate η and step size μ into Theorem 1.

Corollary 1. *Suppose Assumptions 1-5 hold, and let $\mu = (dNHT)^{-\frac{1}{4}}$ and*

$$\eta = N^{\frac{1}{2}}(dHT)^{-\frac{1}{2}} \leq \min \left\{ \frac{N}{72dL}, \frac{2}{NH^2L}, \frac{1}{3\sqrt{dHL}} \right\}, \quad (5)$$

where the inequality can be satisfied if T is large enough. The FedZO algorithm with full device participation satisfies

$$\min_{t \in [T]} \mathbb{E} \|\nabla f(\mathbf{x}^t)\|^2 \leq \mathcal{O} \left(d^{\frac{1}{2}}(NHT)^{-\frac{1}{2}} \right) + \mathcal{O} \left((dNHT)^{-\frac{1}{2}} \right), \quad (6)$$

where the right hand side of (6) is dominated by $\mathcal{O} \left(d^{\frac{1}{2}}(NHT)^{-\frac{1}{2}} \right)$.

Remark 1. *From Corollary 1, we notice that the proposed FedZO algorithm can achieve a convergence rate $\mathcal{O} \left(d^{\frac{1}{2}}(NHT)^{-\frac{1}{2}} \right)$ under condition (5). To attain the same accuracy, compared with the algorithm in [10] with rate $\mathcal{O} \left(d^{\frac{1}{2}}(NT)^{-\frac{1}{2}} \right)$, the number of communication rounds required by the FedZO algorithm can be reduced by a factor of H . According to (5), the largest value of H is $\min \left\{ \mathcal{O} \left(d^{\frac{1}{3}}T^{\frac{1}{3}}N^{-1} \right), \mathcal{O} \left(TN^{-1} \right) \right\}$, which leads to the largest reduction of communication overhead while preserving convergence.*

Remark 2. *From Corollary 1, we observe that the FedZO algorithm achieves linear speedup in terms of the number of local iterates and the number of participating edge devices. Besides, it is worth noting that the convergence rate of the FedZO algorithm relies on the dimension of the model parameter \mathbf{x} . In particular, the FedZO algorithm is \sqrt{d} times slower than its first-order counterpart, i.e., FedAvg. Such degeneration is the same as its centralized counterpart [39], and is the best result that can be achieved based on the gradient estimator in (2) [40].*

B. Partial Device Participation

In this subsection, we show the convergence of the FedZO algorithm with partial device participation. By bounding the minimum squared gradient among the global model sequence, we characterize the convergence of the FedZO algorithm in the following theorem.

Theorem 2. *Suppose Assumptions 1-5 hold and the learning rate satisfies*

$$\eta \leq \min \left\{ \frac{M}{96dL}, \frac{2}{MH^2L}, \frac{1}{3\sqrt{dHL}}, \frac{1}{3\sqrt{MH^3L}} \right\}, \quad (7)$$

the FedZO algorithm with partial device participation satisfies

$$\begin{aligned} \min_{t \in [T]} \mathbb{E} \|\nabla f(\mathbf{x}^t)\|^2 &\leq 4 \frac{f(\mathbf{x}^0) - f_*}{HT\eta} + \eta \frac{32dL}{M} (\sigma_g^2 + 3\sigma_h^2) \\ &+ \eta \frac{36HL\sigma_h^2}{M} + 24\eta HL^3\mu^2 + \frac{dL^2\mu^2}{12} + 4L^2\mu^2. \end{aligned} \quad (8)$$

Proof. Please refer to Appendix B. \square

By comparing (8) with (4), we notice that the third and fourth terms in (8) do not appear in (4). This is because full device participation eliminates the randomness of device sampling, thereby reducing the upper bound of the minimum squared gradient among the global model sequence.

Similarly, the following corollary follows by substituting suitable learning rate η and step size μ into Theorem 2.

Corollary 2. *Suppose Assumptions 1-5 hold, and let $\mu = (MH)^{-\frac{1}{2}}(dT)^{-\frac{1}{4}}$, and*

$$\begin{aligned} \eta &= M^{\frac{1}{2}}(dHT)^{-\frac{1}{2}} \\ &\leq \min \left\{ \frac{M}{96dL}, \frac{2}{MH^2L}, \frac{1}{3\sqrt{dHL}}, \frac{1}{3\sqrt{MH^3L}} \right\}, \end{aligned} \quad (9)$$

where the inequality can be satisfied if T is large enough. If $H \leq d$, then the FedZO algorithm with partial device participation satisfies

$$\begin{aligned} \min_{t \in [T]} \mathbb{E} \|\nabla f(\mathbf{x}^t)\|^2 &\leq \mathcal{O} \left(d^{\frac{1}{2}}(MHT)^{-\frac{1}{2}} \right) \\ &+ \mathcal{O} \left((MH)^{-\frac{1}{2}}(dT)^{-1} \right) + \mathcal{O} \left(d^{\frac{1}{2}}(MH)^{-1}T^{-\frac{1}{2}} \right) \\ &+ \mathcal{O} \left((MH)^{-1}(dT)^{-\frac{1}{2}} \right), \end{aligned} \quad (10)$$

where the right hand side of (10) is dominated by $\mathcal{O} \left(d^{\frac{1}{2}}(MHT)^{-\frac{1}{2}} \right)$.

The convergence rate shown in Corollary 2 implies a linear speedup in terms of the number of local iterates and participating edge devices can be attained, which is similar to Corollary 1. According to (9), we further observe that the number of communication rounds of the FedZO algorithm can be reduced by a factor of H with the order of $\min \left\{ d, \mathcal{O} \left(d^{\frac{1}{3}}T^{\frac{1}{3}}M^{-1} \right), \mathcal{O} \left(TM^{-1} \right) \right\}$.

IV. AIRCOMP-ASSISTED FEDZO ALGORITHM

In this section, we study the implementation of the proposed FedZO algorithm over wireless networks using AirComp, where the edge devices communicate with the central server via wireless fading channels.

In each communication round, both the downlink model dissemination phase and the uplink model uploading phase involve wireless transmissions. As the central server generally has a much greater transmit power than the edge devices, the downlink model dissemination is assumed to be error-free as in most of the existing studies [31]–[35] and we focus on the uplink model uploading.

A. Over-the-Air Aggregation

For the FedZO algorithm, a key observation is that the central server is interested in receiving an average of local model updates of scheduled edge devices rather than each individual one. In particular, at the t -th round, the central server aims to acquire

$$\Delta^t = \frac{1}{|\mathcal{M}_t|} \sum_{i \in \mathcal{M}_t} \Delta_i^t, \quad (11)$$

where $|\mathcal{M}_t|$ denotes cardinality of set \mathcal{M}_t . With conventional OMA schemes, the central server in the t -th round first receives the local model update, e.g., Δ_i^t , from each edge device, and then takes an average to obtain the desired global model update, i.e., Δ^t . However, these schemes may not be spectrum-efficient as the number of required resource blocks or the communication latency linearly increases with the number of participating edge devices. AirComp, as a new non-orthogonal multiple access scheme for scalable transmission, allows all edge devices to concurrently transmit their local model updates and exploits the waveform superposition property to achieve spectrum-efficient model aggregation. The communication resource needed for model uploading using AirComp is independent of the number of participating edge devices. Hence, we adopt AirComp for the aggregation of local model updates in this paper.

Consider a wireless FL system where all edge devices and the server are equipped with a single antenna. Over wireless fading channels, the local model updates transmitted by edge devices suffer from detrimental channel distortion, which in turn degenerates the convergence performance of the AirComp-assisted FedZO algorithm. We thus set a threshold h_{\min} and choose a subset of edge devices $\mathcal{M}_t = \{i \mid |h_i^t| \geq h_{\min}\}$ to participate in the training, where $h_i^t \in \mathbb{C}$ represents the channel coefficient between edge device i and the central server in round t . We assume that h_i^t are independent and identically distributed (i.i.d.) across different edge devices and communication rounds [34], [35]. Note that we can treat the adopted device scheduling strategy as uniform sampling analyzed in Section III-B.

With AirComp, the scheduled edge devices concurrently transmit their precoded model updates, e.g., $\alpha_i^t \Delta_i^t$, to the central server, where α_i^t is the transmit scalar of edge device i at the t -th round. Note that synchronization is required among distributed edge devices as in [31]–[35], which can be realized by sharing a reference-clock across the edge devices [41] or utilizing the timing advance technique commonly adopted in 4G long term evolution (LTE) and 5G new radio (NR) [42]. We assume that the model update vector Δ_i^t of dimension d can be transmitted within one transmission block while the channel coefficient is invariant during one transmission block [31]–[35]. Thus, the aggregated signal received at the central server can be expressed as

$$\mathbf{s}^t = \sum_{i \in \mathcal{M}_t} h_i^t \alpha_i^t \Delta_i^t + \mathbf{n}_t, \quad (12)$$

where $\mathbf{n}_t \sim \mathcal{CN}(0, \sigma_w^2 \mathbf{I}_d)$ represents the additive white Gaussian noise (AWGN) vector at the central server.

B. Transceiver Design

The transmitted signal at each edge device is subject to an energy constraint during one communication round, i.e., $\|\alpha_i^t \Delta_i^t\|^2 \leq dP$, where dP is the total energy of each edge device in one communication round. We assume that the channel state information (CSI) is available at both the central server and edge devices as in [31]–[35]. To meet the energy constraint of each edge device, we set the transmit scalar of device i as

$$\alpha_i^t = \frac{h_{\min}}{h_i^t} \sqrt{\frac{dP}{\Delta_{\max}^t}}, \quad \forall i, \quad (13)$$

where $\Delta_{\max}^t = \max_{i \in \mathcal{M}_t} \|\Delta_i^t\|^2$. The received signal is thus given by

$$\mathbf{s}^t = \sqrt{\frac{dP h_{\min}^2}{\Delta_{\max}^t}} \sum_{i \in \mathcal{M}_t} \Delta_i^t + \mathbf{n}_t. \quad (14)$$

To recover the desired global model update Δ^t in (11) from \mathbf{s}^t in (14), the central server scales \mathbf{s}^t with a receive scalar $\frac{1}{|\mathcal{M}_t|} \sqrt{\frac{\Delta_{\max}^t}{dP h_{\min}^2}}$, and obtains a noisy version of the global model update as follows

$$\mathbf{y}^t = \Delta^t + \tilde{\mathbf{n}}_t, \quad (15)$$

where $\tilde{\mathbf{n}}_t \sim \mathcal{N}\left(0, \frac{\sigma_w^2 \Delta_{\max}^t}{|\mathcal{M}_t|^2 dP h_{\min}^2} \mathbf{I}_d\right)$. To facilitate the transceiver design, each edge device needs to know the maximum of squared norm of local model updates among the participating edge devices, i.e., Δ_{\max}^t , and the instantaneous channel coefficient between itself and the central server, i.e., h_i^t , which can be obtained via feedback from the central server. Before uplink model aggregation, the central server collects the squared norm of local model update $\|\Delta_i^t\|^2$ from each edge device $i \in \mathcal{M}_t$, and then broadcasts Δ_{\max}^t to all edge devices. Besides, the central server estimates and feeds back the channel coefficients to these corresponding edge devices. It is worth noting that the communication overhead introduced by the exchange of these scalars is negligible when compared with the transmission of high-dimensional model parameters.

Remark 3. *Different from most existing studies [17], [31]–[33] that only focus on compensating for channel fading, the adopted transmitter design, i.e., (13), takes the scale of the model update into account. This ensures that the distortion between the obtained signal and the desired signal, i.e., the scaled receiver noise, is proportional to the maximum of the squared norm of local updates. This distortion diminishes when the local model converges. In other words, with such a transmitter design, the detrimental effect of the noise can be eliminated as the iteration proceeds for a convergent algorithm.*

C. Convergence Analysis for AirComp-Assisted FedZO

In the following theorem, we characterize the convergence of the AirComp-assisted FedZO algorithm described in the previous two subsections.

Theorem 3. Suppose that Assumptions 1-5 hold and the learning rate satisfies

$$\eta \leq \min \left\{ \frac{\tilde{M}}{192dL}, \frac{\tilde{M}^2\gamma}{24dNHL}, \frac{3}{2\tilde{M}H^2L}, \frac{1}{3\sqrt{dHL}}, \frac{1}{2\sqrt{3\tilde{M}H^3L}}, \frac{\sqrt{\tilde{M}\gamma}}{L\sqrt{2dNH^3}} \right\}, \quad (16)$$

where $\tilde{M} = \min\{|\mathcal{M}_t|, t \in [T]\}$. The AirComp-assisted FedZO algorithm satisfies

$$\begin{aligned} \min_{t \in [T]} \mathbb{E} \|\nabla f(\mathbf{x}^t)\|^2 &\leq 4 \frac{f(\mathbf{x}^0) - f_*}{HT\eta} + \eta \frac{32dL}{\tilde{M}} (\sigma_g^2 + 3\sigma_h^2) \tilde{C} \\ &+ \eta \frac{36HL\sigma_h^2}{\tilde{M}} + 24\eta HL^3 \mu^2 + \frac{dL^2\mu^2}{12} + 4L^2\mu^2, \end{aligned} \quad (17)$$

where $\tilde{C} = 1 + \frac{NH}{8\tilde{M}\gamma}$ and $\gamma = \frac{Ph_{\min}^2}{\sigma_w^2}$.

As can be observed from Theorem 3, the convergence rate depends on γ , which is the minimum receive SNR. Theorem 3 reduces to Theorem 2 when γ goes to infinity, i.e., noise-free case. Obviously, a smaller value of SNR leads to a slower convergence speed, which meets our intuition. In the following corollary, we show that a convergence rate $\mathcal{O}\left(d^{\frac{1}{2}}(\tilde{M}HT)^{-\frac{1}{2}}\right)$, the same order as the noise-free case presented in Section III-B, can be achieved with appropriate receive SNR γ , learning rate η , and step size μ .

Corollary 3. With $H \leq d$ and $NH \leq 8\tilde{M}\gamma$, let $\mu = (\tilde{M}H)^{-\frac{1}{2}}(dT)^{-\frac{1}{4}}$ and

$$\eta = \tilde{M}^{\frac{1}{2}}(dHT)^{-\frac{1}{2}} \leq \min \left\{ \frac{\tilde{M}}{192dL}, \frac{\tilde{M}^2\gamma}{24dNHL}, \frac{3}{2\tilde{M}H^2L}, \frac{1}{3\sqrt{dHL}}, \frac{1}{2\sqrt{3\tilde{M}H^3L}}, \frac{\sqrt{\tilde{M}\gamma}}{L\sqrt{2dNH^3}} \right\}, \quad (18)$$

we have

$$\begin{aligned} \min_{t \in [T]} \mathbb{E} \|\nabla f(\mathbf{x}^t)\|^2 &\leq \mathcal{O}\left(d^{\frac{1}{2}}(\tilde{M}HT)^{-\frac{1}{2}}\right) \\ &+ \mathcal{O}\left((\tilde{M}H)^{-\frac{1}{2}}(dT)^{-1}\right) + \mathcal{O}\left(d^{\frac{1}{2}}(\tilde{M}H)^{-1}T^{-\frac{1}{2}}\right) \\ &+ \mathcal{O}\left((\tilde{M}H)^{-1}(dT)^{-\frac{1}{2}}\right), \end{aligned} \quad (19)$$

where the right hand side of (19) is dominated by $\mathcal{O}\left(d^{\frac{1}{2}}(\tilde{M}HT)^{-\frac{1}{2}}\right)$.

It is worth noting that the linear speedup in terms of the number of the local iterates and the number of edge devices can still be preserved under appropriate parameter settings.

Remark 4. From Corollary 3, it can be observed that the upper bound of the minimum squared gradient among the global model sequence approaches to zero as T goes to infinity, while that of the existing algorithms with AirComp is only shown to be bounded by a non-diminishing term, known as the optimality gap [31]–[33]. Moreover, the transceiver design in [31]–[33] is transformed to an optimization problem

aiming to minimize the optimality gap, which is computationally expensive. In contrast, our transceiver design follows the principle of COTAF [34] and mitigates the detrimental impact of channel fading and receiver noise perturbation without the need of solving optimization problems. Note that the analysis in [34] concentrates on the first-order algorithm under the strongly convex setup and relies on the assumption of bounded gradients, which are not required in this paper.

V. SIMULATION RESULTS

In this section, we present simulation results to evaluate the effectiveness of the proposed FedZO algorithm for applications of federated black-box attack and softmax regression.

A. Federated Black-Box Attack

The robustness of machine learning (ML) models is an important performance metric for their practical application. For example, in an image classification model, the prediction results of the ML model are expected to be the same as the decision that humans make. In other words, the same output should be generated by a robust model if the input image is perturbed by a noise imperceptible to human. To evaluate the robustness of ML models, black-box attacks can be adopted, where the adversary acts as a standard user that does not have access to the inner structure of ML models and can only query the outputs (label or confidence score) for different inputs. This situation occurs when attacking ML cloud services where the model only serves as an API. Due to the black-box property, the optimization of black-box attacks falls into the category of zeroth-order optimization.

We consider federated black-box attacks [10] on the image classification DNN models that are well trained on some standard datasets. Federated black-box attacks aim to collaboratively generate a common perturbation such that the perturbed images are visually imperceptible to a human but could mislead the classifier. For image \mathbf{z}_i , the attack loss [43] is given by

$$\begin{aligned} \psi_i(\mathbf{x}) &= \max \left\{ \Phi_{y_i} \left(\frac{1}{2} \tanh(\tanh^{-1} 2\mathbf{z}_i + \mathbf{x}) \right) \right. \\ &\quad \left. - \max_{j \neq y_i} \left\{ \Phi_j \left(\frac{1}{2} \tanh(\tanh^{-1} 2\mathbf{z}_i + \mathbf{x}) \right) \right\}, 0 \right\} \\ &\quad + c \left\| \frac{1}{2} \tanh(\tanh^{-1} 2\mathbf{z}_i + \mathbf{x}) - \mathbf{z}_i \right\|^2, \end{aligned}$$

where y_i denotes the label of image \mathbf{z}_i , $\Phi_j(\mathbf{z})$ represents the prediction confidence of image \mathbf{z} to class j , $\frac{1}{2} \tanh(\tanh^{-1} 2\mathbf{z}_i + \mathbf{x})$ is the adversarial example of \mathbf{z}_i , $\frac{1}{2} \tanh(\tanh^{-1} 2\mathbf{z}_i + \mathbf{x}) - \mathbf{z}_i$ is the distortion perturbed by \mathbf{x} in the original image space. The first term of $\psi_i(\mathbf{x})$ measures the probability of failing to attack. The last term of $\psi_i(\mathbf{x})$ represents the distortion induced by \mathbf{x} in the original image space. The goal of attack is to find a visually small perturbation to mislead the classifier $\Phi(\cdot)$ that can be realized by minimizing $\psi_i(\mathbf{x})$. Parameter c balances the tradeoff between the adversarial success and distortion loss. We denote the dataset at edge device n as \mathcal{D}_n . The attack loss of device n can be expressed

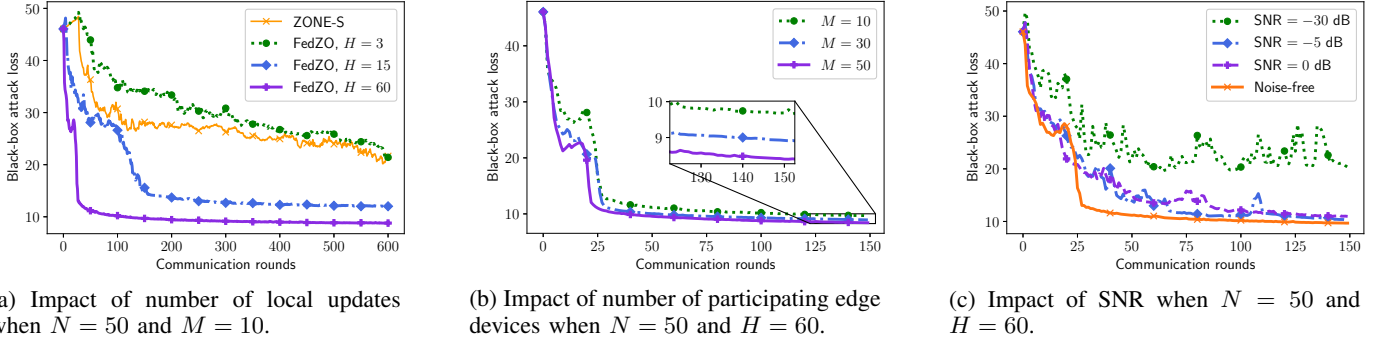


Fig. 1: Federated black-box attack loss versus number of communication rounds.

as $f_n(\mathbf{x}) = \frac{1}{|\mathcal{D}_n|} \sum_{i \in \mathcal{D}_n} \psi_i(x)$. Federated black-box attacks of a DNN model can be formulated as: $\min_{\mathbf{x} \in \mathbb{R}^d} \frac{1}{N} \sum_{n=1}^N f_n(\mathbf{x})$, which can be tackled by the proposed FedZO algorithm.

In this experiment setting, all edge devices share one well-trained DNN classifier¹ that has a testing accuracy of 99.4% on MNIST dataset [43]. We randomly pick 200 samples from the training set of digit class “4”, and then distribute $|\mathcal{D}_n| = 60$ samples to each device n . The number of total edge devices is set to $N = 50$. We set the balancing parameter $c = 1$. The learning rate and step size are set to $\eta_t = 0.02$ and $\mu_t = 0.001$, respectively.

In Fig. 1a, we show the impact of the number of local updates on the convergence performance of the proposed FedZO algorithm with partial device participation when $M = 10$. Specifically, we vary the number of local updates $H \in \{3, 15, 60\}$ and present the attack loss versus the number of communication rounds. It can be observed that the FedZO algorithm can effectively reduce the attack loss for different values of H . Besides, as H increases, the convergence speed of the FedZO algorithm tends to increase. This demonstrates the linear speedup in the number of the local iterates as shown in Section III. We further compare the performance of the proposed FedZO algorithm with ZONE-S [27], which is a state-of-the-art distributed zeroth-order algorithm. Results show that the FedZO algorithm has similar convergence behavior as the ZONE-S algorithm when $H = 3$. With a larger number of local updates, the attack loss of the FedZO algorithm decreases much faster than that of the ZONE-S algorithm, which demonstrates the effectiveness of the FedZO algorithm. It is worth noting that the FedZO algorithm with different values of H in Fig. 1a converges to different losses. This is because the problem of federated black-box attacks on the DNN models is highly non-convex, there exist various saddle points, and the FedZO algorithms may be trapped in any of them.

Fig. 1b shows the convergence performance of the FedZO algorithm versus the number of participating edge devices when $H = 60$. The number of participating edge devices M takes values from set $\{10, 30, 50\}$. It is clear that our proposed algorithm works well in terms of reducing attack loss under the three different values of M . As can be observed, increasing the number of edge devices gives rise to a better convergence

speed. We can observe the linear speedup in the number of participating devices, which matches well with our analysis in Section III.

In Fig. 1c, we show the performance of the AirComp-assisted FedZO algorithm presented in Section IV. Without loss of generality, we model the channel as $h_i^t \sim \mathcal{CN}(0, 1)$, $\forall i, t$, and set the threshold $h_{\min} = 0.8$. Besides, we set the number of local iterates to $H = 60$. We take the FedZO algorithm with noise-free aggregation as benchmark with $H = 60$ and $M = 10$. We plot the attack loss versus the number of communication rounds under different SNR, i.e., $\text{SNR} \in \{-30 \text{ dB}, -5 \text{ dB}, 0 \text{ dB}\}$. As can be observed, the convergence of the FedZO algorithm can be preserved when $\text{SNR} \in \{-5 \text{ dB}, 0 \text{ dB}\}$. Setting a low SNR, e.g., -30 dB , however, may lead to a poor convergence performance. This is because a large noise perturbs the model aggregation, which in turn hinders the convergence of the FedZO algorithm. These observations are in line with our theoretical analysis in Section IV-C.

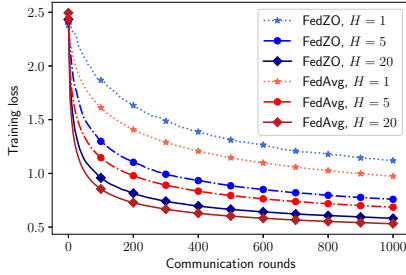
B. Softmax Regression

We further validate our algorithm on the task of softmax regression, which is a classical multi-task classification model. Since the softmax regression can also be solved by using the first-order methods, we compare the FedZO algorithm with the popular FedAvg algorithm [2] to evaluate the effectiveness of our proposed algorithm.

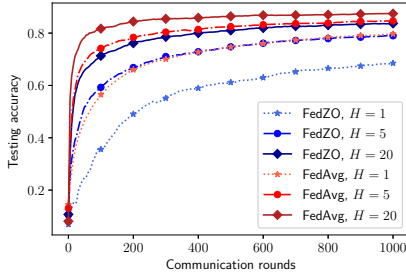
We apply the softmax regression model to a 10-class-classification task on MNIST. In the experiment, we set the number of devices $N = 50$. We sort the samples in the training set according to their labels, and then divide the training set into 120 shards of size 500. We assign two shards to each device, such that each device owns a dataset of 1000 samples. The data available at edge devices are non-i.i.d., and each edge device is assigned with at most four distinctive digit labels.

As shown in Fig. 2, the convergence rate of the FedZO algorithm is slightly slower than that of the FedAvg algorithm under the same number of local updates. This gap is brought by the uncertainty of the gradient estimator that FedZO utilizes. Further, we notice that the FedZO algorithm with $H = 20$ achieves comparable performance as the FedAvg algorithm with $H = 5$. As the FedZO algorithm only relies on the zeroth-order information, the slightly decreased perfor-

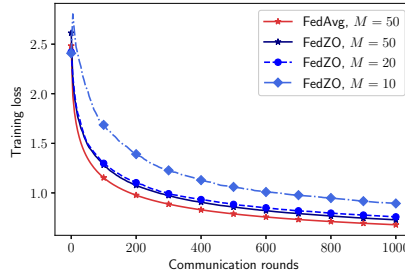
¹https://github.com/carlini/nn_robust_attacks.



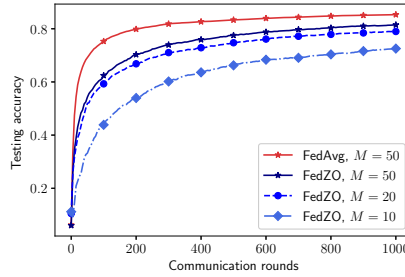
(a) Training loss



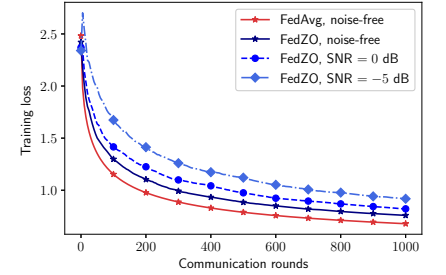
(b) Testing accuracy

Fig. 2: Impact of number of local updates when $N = 50$ and $M = 50$.

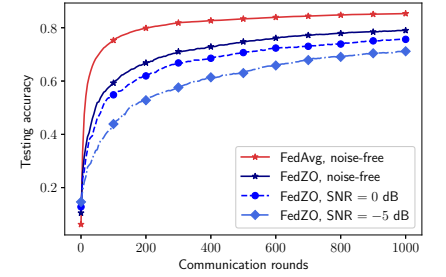
(a) Training loss



(b) Testing accuracy

Fig. 3: Impact of number of participating edge devices when $N = 50$ and $H = 5$.

(a) Training loss



(b) Testing accuracy

Fig. 4: Impact of SNR when $N = 50$ and $H = 5$.

performance is reasonable, and demonstrates the effectiveness of the FedZOO algorithm. This also shows that the FedZOO algorithm can serve as a satisfactory alternative for the FedAvg algorithm when the first-order information is not available.

In Fig. 3, we take the FedAvg algorithm as a benchmark when $H = 5$ and $M = 50$, and further investigate the impact of the number of participating edge devices, i.e., M , on the convergence behaviour of the FedZOO algorithm. The phenomenon of speedup in M can be witnessed in both the training loss and testing accuracy. We observe that the FedZOO algorithm with $H = 5$ and $M = 50$ attains a comparable performance with the FedAvg algorithm.

Fig. 4 shows the performance of the AirComp-assisted FedZOO algorithm over wireless networks with the same channel setting as mentioned in Section V-A. It can be observed that our proposed algorithm converges as the number of communication rounds increases and performs well when the SNR is not very small, e.g., $\text{SNR} \in \{-5 \text{ dB}, 0 \text{ dB}\}$. Results also show that a greater SNR leads to a higher convergence speed. This result fits well with our analysis.

VI. CONCLUSION

In this paper, we developed a derivative-free FedZOO algorithm to handle federated optimization problems without using the gradient and Hessian information. We characterized its convergence rate $O(\sqrt{d/MHT})$ under a non-convex setup, which demonstrates the linear speedup in terms of the number of participating devices and local iterates. Subsequently, we established the convergence guarantee for the AirComp-assisted FedZOO algorithm to support the implementation of the proposed algorithm over wireless networks. Simulation results

demonstrated the effectiveness of the proposed FedZOO algorithm and showed that the proposed FedZOO algorithm could serve as a satisfactory alternative for the FedAvg algorithm. It was also validated that the AirComp-assisted FedZOO algorithm could attain a comparable performance with that of the noise-free case under certain SNR conditions.

APPENDIX

A. Proof of Theorem 1

For notational ease, we denote $\delta_t = \frac{1}{N} \sum_{i=1}^N \sum_{k=0}^{H-1} \mathbb{E} \|\mathbf{x}_i^{(t,k)} - \mathbf{x}^t\|^2$. The proof of Theorem 1 relies on the following two lemmas. The first lemma characterizes how the global loss, i.e., $f(\mathbf{x}^t)$, evolves as the iteration continues.

Lemma 1. *With Assumptions 1-5 and full edge device participation, by letting $\eta \leq \frac{1}{2HL}$, we have*

$$\begin{aligned} \mathbb{E} [f(\mathbf{x}^{t+1})] &\leq f(\mathbf{x}^t) - \left(\frac{\eta H}{2} - \eta^2 \frac{6dHL}{N} \right) \|\nabla f(\mathbf{x}^t)\|^2 \\ &\quad + \left(\eta L^2 + \eta^2 \frac{6dL^3}{N} \right) \delta_t + \eta^2 \frac{2dHL}{N} (3\sigma_h^2 + \sigma_g^2) \\ &\quad + \eta^2 \frac{d^2 HL^3 \mu^2}{2N} + \eta HL^2 \mu^2. \end{aligned} \quad (20)$$

Lemma 1 implies that we need to bound δ_t , which is tackled by the following lemma.

Lemma 2. *With Assumptions 1-5 and $\eta \leq \frac{1}{3HL\sqrt{d}}$, we have*

$$\delta_t \leq 3\eta^2 dH^3 \|\nabla f(\mathbf{x}^t)\|^2 + \eta^2 dH^3 (\sigma_g^2 + 3\sigma_h^2) + \frac{d^2 H^3 L^2}{4} \eta^2 \mu^2.$$

By substituting the upper bound of δ_t in Lemma 2 into (20), we obtain

$$\begin{aligned} \mathbb{E}[f(\mathbf{x}^{t+1})] &\leq f(\mathbf{x}^t) - \left(\frac{\eta H}{2} - \eta^2 \frac{6dHL}{N} - Q_1(\eta)3dH^3\eta^2\right) \|\nabla f(\mathbf{x}^t)\|^2 \\ &\quad + \eta^2 (\sigma_g^2 + 3\sigma_h^2) \left(\frac{2dHL}{N} + Q_1(\eta)dH^3\right) \\ &\quad + Q_1(\eta) \frac{d^2H^3L^2}{4} \eta^2 \mu^2 + \eta^2 \frac{d^2HL^3\mu^2}{2N} + \eta H L^2 \mu^2, \end{aligned}$$

where $Q_1(\eta) = \eta L^2 + \eta^2 \frac{6dL^3}{N}$. Under condition (3), we have $Q_1(\eta)3dH^3 \leq \frac{12dHL}{N}$ and $\eta^2 \frac{18dHL}{N} \leq \frac{\eta H}{4}$, which further lead to $Q_1(\eta) \frac{d^2H^3L^2}{4} \eta^2 \mu^2 \leq \frac{d^2HL^3\eta^2\mu^2}{N}$ and $\frac{3d^2HL^3\eta^2\mu^2}{2N} \leq \frac{\eta dHL^2\mu^2}{48}$. As a result, we obtain

$$\begin{aligned} \mathbb{E}[f(\mathbf{x}^{t+1})] &\leq f(\mathbf{x}^t) - \frac{\eta H}{4} \|\nabla f(\mathbf{x}^t)\|^2 \\ &\quad + \eta^2 \frac{6dHL}{N} (\sigma_g^2 + 3\sigma_h^2) + \frac{\eta dHL^2\mu^2}{48} + \eta H L^2 \mu^2. \end{aligned} \quad (21)$$

By taking an expectation for (21) over \mathbf{x}^t and telescoping from $t = 0$ to $T - 1$, we obtain

$$\begin{aligned} \frac{1}{T} \sum_{t=0}^{T-1} \mathbb{E} \|\nabla f(\mathbf{x}^t)\|^2 &\leq 4 \frac{f(\mathbf{x}^0) - \mathbb{E}[f(\mathbf{x}^T)]}{HT\eta} \\ &\quad + \eta \frac{24dL}{N} (\sigma_g^2 + 3\sigma_h^2) + \frac{dL^2\mu^2}{12} + 4L^2\mu^2. \end{aligned} \quad (22)$$

As $f(\mathbf{x})$ is bounded below, i.e., $f(\mathbf{x}) \geq f_*$, we obtain Theorem 1.

B. Proof of Theorem 2

We first characterize how the global loss, i.e., $f(\mathbf{x}^t)$, evolves as the iteration continues in the following lemma.

Lemma 3. *With Assumptions 1-5 and partial device participation, by letting the learning rate $\eta \leq \frac{1}{2HL}$, we have*

$$\begin{aligned} \mathbb{E}[f(\mathbf{x}^{t+1})] &\leq f(\mathbf{x}^t) - \left(\frac{\eta H}{2} - \eta^2 \frac{6dHL}{M}\right) \|\nabla f(\mathbf{x}^t)\|^2 \\ &\quad + \left(\eta L^2 + \eta^2 \frac{6dL^3}{M} + \eta^2 18HL^3\right) \delta_t + \eta^2 \frac{2dHL}{M} (3\sigma_h^2 + \sigma_g^2) \\ &\quad + \frac{9\eta^2 H^2 L^3 \sigma_h^2}{M} + 6\eta^2 H^2 L^3 \mu^2 + \eta^2 \frac{d^2HL^3\mu^2}{2M} + \eta H L^2 \mu^2. \end{aligned}$$

Combining Lemmas 2 and 3, we have

$$\begin{aligned} \mathbb{E}[f(\mathbf{x}^{t+1})] &\leq f(\mathbf{x}^t) - \left(\frac{\eta H}{2} - \eta^2 \frac{6dHL}{N} - Q_2(\eta)3dH^3\eta^2\right) \|\nabla f(\mathbf{x}^t)\|^2 \\ &\quad + \eta^2 (\sigma_g^2 + 3\sigma_h^2) \left(\frac{2dHL}{M} + Q_2(\eta)dH^3\right) + Q_2(\eta) \frac{d^2H^3L^2}{4} \eta^2 \mu^2 \\ &\quad + \frac{9\eta^2 H^2 L \sigma_h^2}{M} + 6\eta^2 H^2 L^3 \mu^2 + \eta^2 \frac{d^2HL^3\mu^2}{2M} + \eta H L^2 \mu^2. \end{aligned}$$

where $Q_2(\eta) = \eta L^2 + \eta^2 \frac{6dL^3}{M} + \eta^2 18HL^3$. Under condition (7), we have $Q_2(\eta)3dH^3 \leq \frac{18dLH}{M}$ and $\frac{24\eta^2 dLH}{M} \leq \frac{\eta H}{4}$, which further yield $Q_2(\eta) \frac{d^2H^3L^2}{4} \eta^2 \mu^2 \leq \frac{3d^2HL^3\eta^2\mu^2}{2M}$ and $\frac{d^2HL^3\eta^2\mu^2}{M} \leq \frac{\eta\mu^2 HdL^2}{96}$. It follows that

$$\begin{aligned} \mathbb{E}[f(\mathbf{x}^{t+1})] &\leq f(\mathbf{x}^t) - \frac{\eta H}{4} \|\nabla f(\mathbf{x}^t)\|^2 + \eta^2 \frac{8dHL}{M} (\sigma_g^2 + 3\sigma_h^2) \\ &\quad + \frac{9\eta^2 H^2 L \sigma_h^2}{M} + 6\eta^2 H^2 L^3 \mu^2 + \frac{\eta\mu^2 HdL^2}{48} + \eta H L^2 \mu^2. \end{aligned}$$

Following the similar derivation as in Appendix A, we obtain Theorem 2.

C. Proof of Theorem 3

As $\mathbf{x}^{t+1} = \mathbf{x}^t + \frac{1}{|\mathcal{M}_t|} \sum_{i \in \mathcal{M}_t} \Delta_i^t + \tilde{\mathbf{n}}_t$, we have $\mathbf{x}^{t+1} = \tilde{\mathbf{x}}^{t+1} + \tilde{\mathbf{n}}_t$, where $\tilde{\mathbf{x}}^{t+1} = \mathbf{x}^t + \frac{1}{|\mathcal{M}_t|} \sum_{i \in \mathcal{M}_t} \Delta_i^t$ denotes the model with noise-free aggregation. Because of the smoothness of $f(\mathbf{x})$, we obtain

$$f(\mathbf{x}^{t+1}) \leq f(\tilde{\mathbf{x}}^{t+1}) + \langle \nabla f(\tilde{\mathbf{x}}^{t+1}), \tilde{\mathbf{n}}_t \rangle + \frac{L}{2} \|\tilde{\mathbf{n}}_t\|^2. \quad (23)$$

We denote $\beta_t = \frac{1}{N} \sum_{i=1}^N \|\mathbf{x}_i^{(t,H)} - \mathbf{x}^t\|^2$. By taking an expectation over $\tilde{\mathbf{n}}_t$ conditioned on $\tilde{\mathbf{x}}^{t+1}$ and utilizing $\max_i \|\mathbf{x}_i^{(t,H)} - \mathbf{x}^t\|^2 \leq N\beta_t$, we have

$$\mathbb{E}[f(\mathbf{x}^{t+1})] \leq f(\tilde{\mathbf{x}}^{t+1}) + \frac{L}{2\gamma} \frac{N}{|\mathcal{M}_t|^2} \beta_t. \quad (24)$$

The above result suggests that we need to bound β_t , which can be handled by the following lemma.

Lemma 4. *With Assumptions 1-5 hold, we have*

$$\begin{aligned} \beta_t &\leq 6dHL^2\eta^2\delta_t + 6dH^2\eta^2 \|\nabla f(\mathbf{x}^t)\|^2 + 2dH^2\eta^2(\sigma_g^2 + 3\sigma_h^2) \\ &\quad + \frac{d^2H^2L^2}{2} \eta^2 \mu^2. \end{aligned} \quad (25)$$

Combining Lemmas 2, 3, and 4, we obtain

$$\begin{aligned} \mathbb{E}[f(\mathbf{x}^{t+1})] &\leq f(\mathbf{x}^t) - \left(\frac{\eta H}{2} - \eta^2 \tilde{Q}_3(\eta)\right) \|\nabla f(\mathbf{x}^t)\|^2 \\ &\quad + \eta^2 (\sigma_g^2 + 3\sigma_h^2) \frac{\tilde{Q}_3(\eta)}{3} + \frac{9\eta^2 H^2 L \sigma_h^2}{|\mathcal{M}_t|} + \frac{B_0 d L \eta^2 \mu^2}{12} + \frac{d^2 N H^2 L^3}{4 |\mathcal{M}_t|^2 \gamma} \eta^2 \mu^2 \\ &\quad + 6H^2 L^3 \eta^2 \mu^2 + \frac{d^2 H L^3 \eta^2 \mu^2}{2 |\mathcal{M}_t|} + H L^2 \eta \mu^2, \end{aligned}$$

where $\tilde{Q}_3(\eta) = \frac{6dHL}{|\mathcal{M}_t|} + \frac{3dNH^2L}{|\mathcal{M}_t|^2\gamma} + Q_3(\eta)$ and

$$Q_3(\eta) = \left(\eta L^2 + \eta^2 \frac{6dL^3}{|\mathcal{M}_t|} + \eta^2 18HL^3 + \frac{3dNH^2L^3\eta^2}{|\mathcal{M}_t|^2\gamma}\right) 3dH^3.$$

Under condition (16), we have $\frac{3dNH^2L\eta^2}{|\mathcal{M}_t|^2\gamma} \leq \frac{\eta H}{8}$, $Q_3(\eta) \leq \frac{18dHL}{|\mathcal{M}_t|}$, and $\eta^2 \frac{24dHL}{|\mathcal{M}_t|} \leq \frac{\eta H}{8}$, which further lead to $\frac{Q_3(\eta)dL\eta^2\mu^2}{12} \leq \frac{3d^2HL^3}{2|\mathcal{M}_t|} \eta^2 \mu^2$, $\frac{2d^2HL^3\eta^2\mu^2}{|\mathcal{M}_t|} \leq \frac{\eta\mu^2 HdL^2}{96}$, and $\frac{d^2NH^2L^3}{4|\mathcal{M}_t|^2\gamma} \eta^2 \mu^2 \leq \frac{\eta\mu^2 HdL^2}{96}$. Hence, we obtain

$$\begin{aligned} \mathbb{E}[f(\mathbf{x}^{t+1})] &\leq f(\mathbf{x}^t) - \frac{\eta H}{4} \|\nabla f(\mathbf{x}^t)\|^2 + \eta^2 \frac{8dHL}{|\mathcal{M}_t|} (\sigma_g^2 + 3\sigma_h^2) \\ &\quad + \eta^2 \frac{dNH^2L}{|\mathcal{M}_t|^2\gamma} (\sigma_g^2 + 3\sigma_h^2) + \frac{9\eta^2 H^2 L \sigma_h^2}{|\mathcal{M}_t|} \\ &\quad + 6\eta^2 H^2 L^3 \mu^2 + \frac{\eta\mu^2 HdL^2}{48} + \eta H L^2 \mu^2. \end{aligned} \quad (26)$$

After reorganizing (26), we obtain

$$\begin{aligned} \|\nabla f(\mathbf{x}^t)\|^2 &\leq 4 \frac{f(\mathbf{x}^t) - \mathbb{E}[f(\mathbf{x}^{t+1})]}{\eta H} + \eta \frac{32dL}{|\mathcal{M}_t|} (\sigma_g^2 + 3\sigma_h^2) \hat{C} \\ &\quad + \frac{36\eta HL \sigma_h^2}{|\mathcal{M}_t|} + 24\eta HL^3 \mu^2 + \frac{dL^2\mu^2}{12} + 4L^2\mu^2, \end{aligned} \quad (27)$$

where $\hat{C} = 1 + \frac{NH}{8\tilde{M}\gamma}$ with $\tilde{M} \leq |\mathcal{M}_t|$, $\forall t$. Following the similar derivation as in Appendix A, we obtain Theorem 3.

D. Proof of Lemmas

As the proof of Lemma 1 is a simplified version of that of Lemma 3. Before proving Lemma 1, we first prove Lemma 3.

1) *Proof of Lemma 3:* For notational ease, we denote $\mathbf{e}_i^{(t,k)} = \widetilde{\nabla}_v^\mu F_i(\mathbf{x}_i^{(t,k)}, \xi_i^{(t,k)})$. Because of $\frac{1}{M} \sum_{i \in \mathcal{M}_t} \sum_{k=0}^{H-1} \mathbf{e}_i^{(t,k)} = \mathbf{x}^{t+1} - \mathbf{x}^t$ and the smoothness of $f(\mathbf{x})$, we obtain

$$f(\mathbf{x}^{t+1}) \leq f(\mathbf{x}^t) - \eta \left\langle \nabla f(\mathbf{x}^t), \frac{1}{M} \sum_{i \in \mathcal{M}_t} \sum_{k=0}^{H-1} \mathbf{e}_i^{(t,k)} \right\rangle + \eta^2 \frac{L}{2} \left\| \frac{1}{M} \sum_{i \in \mathcal{M}_t} \sum_{k=0}^{H-1} \mathbf{e}_i^{(t,k)} \right\|^2. \quad (28)$$

By taking expectation for (28) over $\{\mathcal{M}_t, \{\xi_i^{(t,k)}, v^{(t,k)}\}, \forall i, k\}$, conditioned on \mathbf{x}^t , we obtain

$$\mathbb{E}[f(\mathbf{x}^{t+1})] \leq f(\mathbf{x}^t) - \eta \underbrace{\mathbb{E} \left\langle \nabla f(\mathbf{x}^t), \frac{1}{M} \sum_{i \in \mathcal{M}_t} \sum_{k=0}^{H-1} \mathbf{e}_i^{(t,k)} \right\rangle}_{T_1} + \eta^2 \frac{L}{2} \underbrace{\mathbb{E} \left\| \frac{1}{M} \sum_{i \in \mathcal{M}_t} \sum_{k=0}^{H-1} \mathbf{e}_i^{(t,k)} \right\|^2}_{T_2}. \quad (29)$$

We next bound T_1 and T_2 . As \mathcal{M}_t is uniformly sampled from N edge devices, we have [21, Lemma 4]

$$T_1 = -\eta \mathbb{E} \left\langle \nabla f(\mathbf{x}^t), \frac{1}{N} \sum_{i=1}^N \sum_{k=0}^{H-1} \mathbf{e}_i^{(t,k)} \right\rangle.$$

According to the properties of gradient estimator that [44, Lemma 4.2]

$$\mathbb{E}[\mathbf{e}_i^{(t,k)}] = \nabla f_i^\mu(\mathbf{x}_i^{(t,k)}), \quad (30)$$

we have

$$T_1 = -\eta \mathbb{E} \left\langle \nabla f(\mathbf{x}^t), \frac{1}{N} \sum_{i=1}^N \sum_{k=0}^{H-1} \nabla f_i^\mu(\mathbf{x}_i^{(t,k)}) \right\rangle,$$

where $f_i^\mu(\mathbf{x}) = \mathbb{E}_{\mathbf{u} \sim \mathcal{U}(\mathbb{B}_d)}[f(\mathbf{x} + \mu \mathbf{u})]$ is a locally averaged version of $f(\mathbf{x})$ [44]. According to the basic identity, we have

$$T_1 = -\frac{\eta H}{2} \|\nabla f(\mathbf{x}^t)\|^2 - \frac{\eta H}{2} \mathbb{E} \left\| \frac{1}{NH} \sum_{i=1}^N \sum_{k=0}^{H-1} \nabla f_i^\mu(\mathbf{x}_i^{(t,k)}) \right\|^2 + \frac{\eta H}{2} \underbrace{\mathbb{E} \left\| \frac{1}{NH} \sum_{i=1}^N \sum_{k=0}^{H-1} (\nabla f_i^\mu(\mathbf{x}_i^{(t,k)}) - \nabla f_i(\mathbf{x}^t)) \right\|^2}_{T_3},$$

For T_3 , we have

$$\begin{aligned} T_3 &= \mathbb{E} \left\| \frac{1}{NH} \sum_{i=1}^N \sum_{k=0}^{H-1} (\nabla f_i^\mu(\mathbf{x}_i^{(t,k)}) - \nabla f_i(\mathbf{x}^t)) \right\|^2 \\ &\leq \frac{1}{NH} \sum_{i=1}^N \sum_{k=0}^{H-1} \mathbb{E} \|\nabla f_i^\mu(\mathbf{x}_i^{(t,k)}) \mp \nabla f_i(\mathbf{x}_i^{(t,k)}) - \nabla f_i(\mathbf{x}^t)\|^2 \\ &\leq \frac{2}{NH} \sum_{i=1}^N \sum_{k=0}^{H-1} \mathbb{E} \|\nabla f_i^\mu(\mathbf{x}_i^{(t,k)}) - \nabla f_i(\mathbf{x}_i^{(t,k)})\|^2 \\ &\quad + \frac{2}{NH} \sum_{i=1}^N \sum_{k=0}^{H-1} \mathbb{E} \|\nabla f_i(\mathbf{x}_i^{(t,k)}) - \nabla f_i(\mathbf{x}^t)\|^2 \\ &\leq 2L^2 \mu^2 + \frac{2L^2}{NH} \sum_{i=1}^N \sum_{k=0}^{H-1} \mathbb{E} \|\mathbf{x}_i^{(t,k)} - \mathbf{x}^t\|^2, \end{aligned} \quad (31)$$

where the first inequality follows by Jensen's inequality, the second inequality holds because of Cauchy-Schwartz inequality, and the last inequality follows by [28, Lemma 5.2] and smoothness of $f_i(\mathbf{x})$. Plugging (31) into (31), it follows that

$$T_1 \leq -\frac{\eta H}{2} \|\nabla f(\mathbf{x}^t)\|^2 - \frac{\eta H}{2} \mathbb{E} \left\| \frac{1}{NH} \sum_{i=1}^N \sum_{k=0}^{H-1} \nabla f_i^\mu(\mathbf{x}_i^{(t,k)}) \right\|^2 + \eta H L^2 \mu^2 + \eta H L^2 \frac{1}{NH} \sum_{i=1}^N \sum_{k=0}^{H-1} \mathbb{E} \|\mathbf{x}_i^{(t,k)} - \mathbf{x}^t\|^2. \quad (32)$$

For T_2 , according to Cauchy-Schwartz inequality, we have

$$T_2 \leq 2 \mathbb{E} \left\| \underbrace{\frac{1}{M} \sum_{i \in \mathcal{M}_t} \sum_{k=0}^{H-1} (\mathbf{e}_i^{(t,k)} - \nabla f_i^\mu(\mathbf{x}_i^{(t,k)}))}_{T_4} \right\|^2 + 2 \mathbb{E} \left\| \underbrace{\frac{1}{M} \sum_{i \in \mathcal{M}_t} \sum_{k=0}^{H-1} \nabla f_i^\mu(\mathbf{x}_i^{(t,k)})}_{T_5} \right\|^2. \quad (33)$$

By denoting $\mathbf{h}_i = \sum_{k=0}^{H-1} (\mathbf{e}_i^{(t,k)} - \nabla f_i^\mu(\mathbf{x}_i^{(t,k)}))$ and recalling (30), we have $\mathbb{E}[\mathbf{h}_i] = \mathbf{0}$. Due to the independence between edge devices i and j , $\forall j \neq i$, we have $\mathbb{E}\langle \mathbf{h}_i, \mathbf{h}_j \rangle = 0$. We thus obtain

$$T_4 = \frac{1}{M^2} \mathbb{E}_{\mathcal{M}_t} \sum_{i \in \mathcal{M}_t} \mathbb{E} \left\| \sum_{k=0}^{H-1} (\mathbf{e}_i^{(t,k)} - \nabla f_i^\mu(\mathbf{x}_i^{(t,k)})) \right\|^2.$$

Besides, by utilizing

$$\mathbb{E} \left[\mathbf{e}_i^{(t,k)} - \nabla f_i^\mu(\mathbf{x}_i^{(t,k)}) \mid \{\mathbf{x}_i^{(t,k')}\}_{k'=0}^k \right] = 0,$$

and the law of total expectation [7, Lemma 2], we have

$$T_4 = \frac{1}{M^2} \mathbb{E}_{\mathcal{M}_t} \sum_{i \in \mathcal{M}_t} \sum_{k=0}^{H-1} \mathbb{E} \left\| \mathbf{e}_i^{(t,k)} - \nabla f_i^\mu(\mathbf{x}_i^{(t,k)}) \right\|^2. \quad (34)$$

We further bound T_4 as

$$\begin{aligned} T_4 &\leq \frac{1}{M^2} \mathbb{E}_{\mathcal{M}_t} \sum_{i \in \mathcal{M}_t} \sum_{k=0}^{H-1} \mathbb{E} \|\mathbf{e}_i^{(t,k)}\|^2 = \frac{1}{MN} \sum_{i=1}^N \sum_{k=0}^{H-1} \mathbb{E} \|\mathbf{e}_i^{(t,k)}\|^2 \\ &\leq \frac{1}{MN} \sum_{i=1}^N \sum_{k=0}^{H-1} \left[2d \mathbb{E} \|\nabla F_i(\mathbf{x}_i^{(t,k)}, \xi_i^{(t,k)})\|^2 + \frac{1}{2} d^2 L^2 \mu^2 \right] \\ &\leq 2d \frac{1}{MN} \sum_{i=1}^N \sum_{k=0}^{H-1} \underbrace{\mathbb{E} \|\nabla f_i(\mathbf{x}_i^{(t,k)})\|^2}_{T_6} + \frac{2dH\sigma_g^2}{M} + \frac{d^2 HL^2 \mu^2}{2M}, \end{aligned} \quad (35)$$

where the equality follows by [21, Lemma 4], the first inequality holds due to $\mathbb{E}\|\mathbf{z}\|^2 \geq \mathbb{E}\|\mathbf{z} - \mathbb{E}\mathbf{z}\|^2$, the second inequality follows by [44, Lemma 4.1], and the last inequality follows by Assumption 4. We further bound T_6 as

$$\begin{aligned} T_6 &= \mathbb{E} \|\nabla f_i(\mathbf{x}_i^{(t,k)}) \mp \nabla f_i(\mathbf{x}^t) \mp \nabla f(\mathbf{x}^t)\|^2 \\ &\leq 3L^2 \mathbb{E} \|\mathbf{x}_i^{(t,k)} - \mathbf{x}^t\|^2 + 3\sigma_h^2 + 3 \|\nabla f(\mathbf{x}^t)\|^2, \end{aligned} \quad (36)$$

where $a \mp b$ represents $a - b + b$ and the inequality follows by the Cauchy-Schwartz inequality, the smoothness of $f_i(\mathbf{x})$, and Assumption 5. Plugging (36) into (35), we obtain

$$\begin{aligned} T_4 &\leq \frac{6dL^2}{M} \mathbb{E} \frac{1}{N} \sum_{i=1}^N \sum_{k=0}^{H-1} \|\mathbf{x}_i^{(t,k)} - \mathbf{x}^t\|^2 + \frac{6dH}{M} \|\nabla f(\mathbf{x}^t)\|^2 \\ &\quad + \frac{2dH}{M} (3\sigma_h^2 + \sigma_g^2) + \frac{d^2 HL^2 \mu^2}{2M}. \end{aligned} \quad (37)$$

As $\mathbb{E}\|z\|^2 = \|\mathbb{E}z\|^2 + \mathbb{E}\|z - \mathbb{E}z\|^2$, we expand T_5 as

$$T_5 = \mathbb{E} \left[\mathbb{E}_{\mathcal{M}_t} \left\| \underbrace{\frac{1}{M} \sum_{i \in \mathcal{M}_t} \sum_{k=0}^{H-1} \nabla f_i^\mu(\mathbf{x}_i^{(t,k)}) - \frac{1}{N} \sum_{i=1}^N \sum_{k=0}^{H-1} \nabla f_i^\mu(\mathbf{x}_i^{(t,k)})}_{T_7} \right\|^2 + \left\| \frac{1}{N} \sum_{i=1}^N \sum_{k=0}^{H-1} \nabla f_i^\mu(\mathbf{x}_i^{(t,k)}) \right\|^2 \right]. \quad (38)$$

For T_7 , we have

$$T_7 = \left\| \frac{1}{M} \sum_{i \in \mathcal{M}_t} \sum_{k=0}^{H-1} \nabla f_i^\mu(\mathbf{x}_i^{(t,k)}) \mp \frac{1}{M} \sum_{i \in \mathcal{M}_t} \sum_{k=0}^{H-1} \nabla f_i(\mathbf{x}_i^{(t,k)}) \mp \frac{1}{N} \sum_{i=1}^N \sum_{k=0}^{H-1} \nabla f_i(\mathbf{x}_i^{(t,k)}) - \frac{1}{N} \sum_{i=1}^N \sum_{k=0}^{H-1} \nabla f_i^\mu(\mathbf{x}_i^{(t,k)}) \right\|^2.$$

By Cauchy-Schwartz inequality, we thus have

$$T_7 \leq 3 \left\| \frac{1}{M} \sum_{i \in \mathcal{M}_t} \sum_{k=0}^{H-1} (\nabla f_i^\mu(\mathbf{x}_i^{(t,k)}) - \nabla f_i(\mathbf{x}_i^{(t,k)})) \right\|^2 + 3 \left\| \frac{1}{M} \sum_{i \in \mathcal{M}_t} \sum_{k=0}^{H-1} \nabla f_i(\mathbf{x}_i^{(t,k)}) - \frac{1}{N} \sum_{i=1}^N \sum_{k=0}^{H-1} \nabla f_i(\mathbf{x}_i^{(t,k)}) \right\|^2 + 3 \left\| \frac{1}{N} \sum_{i=1}^N \sum_{k=0}^{H-1} (\nabla f_i(\mathbf{x}_i^{(t,k)}) - \nabla f_i^\mu(\mathbf{x}_i^{(t,k)})) \right\|^2.$$

Utilizing Jensen's inequality and [28, Lemma 5.2], we obtain

$$T_7 \leq 3 \left\| \underbrace{\frac{1}{M} \sum_{i \in \mathcal{M}_t} \sum_{k=0}^{H-1} \nabla f_i(\mathbf{x}_i^{(t,k)}) - \frac{1}{N} \sum_{i=1}^N \sum_{k=0}^{H-1} \nabla f_i(\mathbf{x}_i^{(t,k)})}_{T_8} \right\|^2 + 6H^2L^2\mu^2. \quad (39)$$

By plugging $\mp \frac{1}{M} \sum_{i \in \mathcal{M}_t} \sum_{k=0}^{H-1} \nabla f_i(\mathbf{x}_i^{(t,k)})$ and $\mp \frac{1}{N} \sum_{i=1}^N \sum_{k=0}^{H-1} \nabla f_i(\mathbf{x}_i^{(t,k)})$ into T_8 , and following a similar derivation for bounding T_7 , we obtain

$$\mathbb{E}_{\mathcal{M}_t}[T_8] \leq 18HL^2 \frac{1}{N} \sum_{i=1}^N \sum_{k=0}^{H-1} \|\mathbf{x}_i^{(t,k)} - \mathbf{x}^t\|^2 + 9H^2 \mathbb{E}_{\mathcal{M}_t} \left\| \underbrace{\frac{1}{M} \sum_{i \in \mathcal{M}_t} \nabla f_i(\mathbf{x}^t) - \nabla f(\mathbf{x}^t)}_{T_9} \right\|^2, \quad (40)$$

where we utilize

$$\mathbb{E}_{\mathcal{M}_t} \frac{1}{M} \sum_{i \in \mathcal{M}_t} \sum_{k=0}^{H-1} \|\mathbf{x}_i^{(t,k)} - \mathbf{x}^t\|^2 = \frac{1}{N} \sum_{i=1}^N \sum_{k=0}^{H-1} \|\mathbf{x}_i^{(t,k)} - \mathbf{x}^t\|^2.$$

For T_9 , we have

$$T_9 = \mathbb{E}_{\mathcal{M}_t} \left\| \frac{1}{M} \sum_{i \in \mathcal{M}_t} (\nabla f_i(\mathbf{x}^t) - \nabla f(\mathbf{x}^t)) \right\|^2 = \frac{1}{M^2} \mathbb{E}_{\mathcal{M}_t} \sum_{i \in \mathcal{M}_t} \|\nabla f_i(\mathbf{x}^t) - \nabla f(\mathbf{x}^t)\|^2 \leq \frac{\sigma_h^2}{M}, \quad (41)$$

where the second identity follows by the independence between the elements of \mathcal{M}_t and $\mathbb{E}_i[\nabla f_i(\mathbf{x}^t)] = \nabla f(\mathbf{x}^t)$, and the last inequality comes from Assumption 5.

Combining (38), (39), (40), and (41), we can bound T_5 as

$$T_5 \leq 18HL^2 \frac{1}{N} \sum_{i=1}^N \sum_{k=0}^{H-1} \mathbb{E} \|\mathbf{x}_i^{(t,k)} - \mathbf{x}^t\|^2 + \frac{9H^2\sigma_h^2}{M} + 6H^2L^2\mu^2 + \mathbb{E} \left\| \frac{1}{N} \sum_{i=1}^N \sum_{k=0}^{H-1} \nabla f_i^\mu(\mathbf{x}_i^{(t,k)}) \right\|^2. \quad (42)$$

Combining (29), (32), (33), (37), and (42), we can obtain Lemma 3.

2) *Proof of Lemma 1:* With full device participation, i.e., $M = N$, we have

$$T_5 = \mathbb{E} \left\| \frac{1}{N} \sum_{i=1}^N \sum_{k=0}^{H-1} \nabla f_i^\mu(\mathbf{x}_i^{(t,k)}) \right\|^2. \quad (43)$$

Combining (29), (32), (33), (37), and (43), we can obtain Lemma 1.

3) *Proof of Lemma 2:* We denote $\frac{1}{N} \sum_{i=1}^N \mathbb{E} \|\mathbf{x}_i^{(t,k)} - \mathbf{x}^t\|^2$ as $s^{(t,k)}$. Recalling the iterate, we have

$$s^{(t,\tau)} = \eta^2 \frac{1}{N} \sum_{i=1}^N \mathbb{E} \left\| \sum_{k=0}^{\tau-1} \mathbf{e}_i^{(t,k)} \right\|^2 \leq \tau \eta^2 \sum_{k=0}^{\tau-1} \frac{1}{N} \sum_{i=1}^N \mathbb{E} \|\mathbf{e}_i^{(t,k)}\|^2,$$

where the inequality follows by Cauchy-Schwartz inequality. Recalling the relations in (35) and (37), we obtain

$$s^{(t,\tau)} \leq 6dL^2\tau\eta^2 \sum_{k=0}^{\tau-1} s^{(t,k)} + 6d\tau^2\eta^2 \|\nabla f(\mathbf{x}^t)\|^2 + 2d\tau^2\eta^2(\sigma_g^2 + 3\sigma_h^2) + \frac{d^2L^2\tau^2}{2}\eta^2\mu^2. \quad (44)$$

Taking summation over τ from 1 to $H-1$, we obtain

$$\sum_{\tau=1}^{H-1} s^{(t,\tau)} \leq 6dL^2\eta^2 \sum_{\tau=1}^{H-1} \tau \sum_{k=0}^{\tau-1} s^{(t,k)} + C \leq 3dH^2L^2\eta^2 \sum_{k=0}^{H-1} s^{(t,k)} + C, \quad (45)$$

where we utilize the property of arithmetic sequence and

$$C = 2dH^3\eta^2 \|\nabla f(\mathbf{x}^t)\|^2 + \frac{2}{3}dH^3\eta^2(\sigma_g^2 + 3\sigma_h^2) + \frac{d^2H^3L^2}{6}\eta^2\mu^2.$$

Utilizing $s^{(t,0)} = 0$ and rearranging (45), we have

$$(1 - 3dH^2L^2\eta^2) \sum_{\tau=0}^{H-1} s^{(t,\tau)} \leq 2dH^3\eta^2 \|\nabla f(\mathbf{x}^t)\|^2 + \frac{2}{3}dH^3\eta^2(\sigma_g^2 + 3\sigma_h^2) + \frac{d^2H^3L^2}{6}\eta^2\mu^2. \quad (46)$$

As $\eta \leq \frac{1}{3HL\sqrt{d}}$, we have $3(1 - 3dH^2L^2\eta^2) \geq 2$. We thus obtain Lemma 2.

4) *Proof of Lemma 4:* Lemma 4 is a byproduct of the derivation of Lemma 2. It can be directly derived from (44).

REFERENCES

- [1] K. B. Letaief, Y. Shi, J. Lu, and J. Lu, "Edge artificial intelligence for 6G: Vision, enabling technologies, and applications," *IEEE J. Sel. Areas Commun.*, pp. 1–1, 2021, doi:10.1109/JSAC.2021.3126076.
- [2] B. McMahan, E. Moore, D. Ramage, S. Hampson, and B. A. y. Arcas, "Communication-Efficient Learning of Deep Networks from Decentralized Data," in *Proc. Int. Conf. Artif. Intell. Stat. (AISTATS)*, 2017.
- [3] Y. Shi, K. Yang, Z. Yang, and Y. Zhou, *Mobile Edge Artificial Intelligence: Opportunities and Challenges*. Elsevier, 2021.
- [4] Y. Qiang, "Federated recommendation systems," in *Proc. IEEE Int. Conf. Big Data*, 2019.
- [5] K. Yang, Y. Shi, Y. Zhou, Z. Yang, L. Fu, and W. Chen, "Federated machine learning for intelligent IoT via reconfigurable intelligent surface," *IEEE Netw.*, vol. 34, no. 5, pp. 16–22, Sept. 2020.
- [6] X. Zhang, M. Hong, S. Dhople, W. Yin, and Y. Liu, "FedPD: A federated learning framework with adaptivity to non-IID data," *IEEE Trans. Signal Process.*, vol. 69, pp. 6055–6070, Oct. 2021.
- [7] J. Wang, Q. Liu, H. Liang, G. Joshi, and H. V. Poor, "A novel framework for the analysis and design of heterogeneous federated learning," *IEEE Trans. Signal Process.*, vol. 69, pp. 5234–5249, 2021.
- [8] T. Li, A. K. Sahu, M. Zaheer, M. Sanjabi, A. Talwalkar, and V. Smithy, "FedDANE: A federated newton-type method," in *Proc. IEEE Asilomar Conf. Signals, Systems, Computers (ACSSC)*, 2019.
- [9] Z. Dai, B. K. H. Low, and P. Jaillet, "Federated bayesian optimization via thompson sampling," in *Proc. Neural Inf. Process. Syst. (NeurIPS)*, 2020.
- [10] X. Yi, S. Zhang, T. Yang, T. Chai, and K. H. Johansson, "Zeroth-order algorithms for stochastic distributed nonconvex optimization," *arXiv preprint arXiv:2106.02958*, 2021. [Online]. Available: <https://arxiv.org/pdf/2106.02958.pdf>
- [11] M. Chen, Z. Yang, W. Saad, C. Yin, H. V. Poor, and S. Cui, "A joint learning and communications framework for federated learning over wireless networks," *IEEE Trans. Wireless Commun.*, vol. 20, no. 1, pp. 269–283, Jan. 2021.
- [12] J. Ren, Y. He, D. Wen, G. Yu, K. Huang, and D. Guo, "Scheduling for cellular federated edge learning with importance and channel awareness," *IEEE Trans. Wireless Commun.*, vol. 19, no. 11, pp. 7690–7703, Nov. 2020.
- [13] Z. Wang, Y. Shi, Y. Zhou, H. Zhou, and N. Zhang, "Wireless-powered over-the-air computation in intelligent reflecting surface-aided IoT networks," *IEEE Internet Things J.*, vol. 8, no. 3, pp. 1585–1598, 2021.
- [14] G. Zhu, J. Xu, K. Huang, and S. Cui, "Over-the-air computing for wireless data aggregation in massive IoT," *IEEE Wirel. Commun.*, vol. 28, no. 4, pp. 57–65, Aug. 2021.
- [15] M. Fu, Y. Zhou, Y. Shi, W. Chen, and R. Zhang, "UAV aided over-the-air computation," *IEEE Trans. Commun.*, pp. 1–1, 2021, doi:10.1109/TWC.2021.3134327.
- [16] W. Fang, Y. Jiang, Y. Shi, Y. Zhou, W. Chen, and K. B. Letaief, "Over-the-air computation via reconfigurable intelligent surface," *IEEE Trans. Commun.*, vol. 69, no. 12, pp. 8612–8626, Dec. 2021.
- [17] K. Yang, T. Jiang, Y. Shi, and Z. Ding, "Federated learning via over-the-air computation," *IEEE Trans. Wireless Commun.*, vol. 19, no. 3, pp. 2022–2035, Mar. 2020.
- [18] M. M. Amiri and D. Gündüz, "Machine learning at the wireless edge: Distributed stochastic gradient descent over-the-air," *IEEE Trans. Signal Process.*, vol. 68, pp. 2155–2169, Mar. 2020.
- [19] G. Zhu, Y. Wang, and K. Huang, "Broadband analog aggregation for low-latency federated edge learning," *IEEE Trans. Wireless Commun.*, vol. 19, no. 1, pp. 491–506, Jan. 2020.
- [20] F. Zhou and G. Cong, "On the convergence properties of a K-step averaging stochastic gradient descent algorithm for nonconvex optimization," in *Proc. Int. Joint Conf. Artif. Intell. (IJCAI)*, 2018.
- [21] X. Li, K. Huang, W. Yang, S. Wang, and Z. Zhang, "On the convergence of FedAvg on Non-IID data," in *Proc. Int. Conf. Learn. Representations (ICLR)*, 2020.
- [22] J. Wang, Z. Charles, Z. Xu, G. Joshi, H. B. McMahan, M. Al-Shedivat, G. Andrew, S. Avestimehr, K. Daly, D. Data *et al.*, "A field guide to federated optimization," *arXiv preprint arXiv:2107.06917*, 2021. [Online]. Available: <https://arxiv.org/pdf/2107.06917.pdf>
- [23] T. Li, A. K. Sahu, M. Zaheer, M. Sanjabi, A. Talwalkar, and V. Smith, "Federated optimization in heterogeneous networks," in *Proc. Mach. Learn. Syst. (MLSys)*, 2020.
- [24] S. P. Karimireddy, S. Kale, M. Mohri, S. J. Reddi, S. U. Stich, and A. T. Suresh, "SCAFFOLD: stochastic controlled averaging for federated learning," in *Proc. Int. Conf. Mach. Learn. (ICML)*, 2020.
- [25] R. Pathak and M. J. Wainwright, "Fedsplit: an algorithmic framework for fast federated optimization," in *Proc. Neural Inf. Process. Syst. (NeurIPS)*, 2020.
- [26] S. Wang, F. Roosta-Khorasani, P. Xu, and M. W. Mahoney, "GIANT: Globally improved approximate newton method for distributed optimization," in *Proc. Neural Inf. Process. Syst. (NeurIPS)*. Red Hook, NY, USA: Curran Associates Inc., 2018.
- [27] D. Hajinezhad, M. Hong, and A. Garcia, "ZONE: Zeroth-order non-convex multiagent optimization over networks," *IEEE Trans. Automat. Contr.*, vol. 64, no. 10, pp. 3995–4010, Oct. 2019.
- [28] Y. Tang, J. Zhang, and N. Li, "Distributed zero-order algorithms for nonconvex multiagent optimization," *IEEE Trans. Control. Netw. Syst.*, vol. 8, no. 1, pp. 269–281, Mar. 2021.
- [29] Z. Li and L. Chen, "Communication-efficient decentralized zeroth-order method on heterogeneous data," in *Int. Conf. Wirel. Commun. Signal Process. (WCSP)*, Changsha, China, 2021, pp. 1–6.
- [30] A. Khaled, K. Mishchenko, and P. Richtárik, "Tighter theory for local SGD on identical and heterogeneous data," in *Proc. Int. Conf. Artif. Intell. Stat. (AISTATS)*, S. Chiappa and R. Calandra, Eds., 2020.
- [31] H. Liu, X. Yuan, and Y.-J. A. Zhang, "Reconfigurable intelligent surface enabled federated learning: A unified communication-learning design approach," *IEEE Trans. Wireless Commun.*, vol. 20, no. 11, pp. 7595–7609, Nov. 2021.
- [32] X. Cao, G. Zhu, J. Xu, Z. Wang, and S. Cui, "Optimized power control design for over-the-air federated edge learning," *IEEE J. Sel. Areas Commun.*, pp. 1–1, 2021, doi:10.1109/JSAC.2021.3126060.
- [33] Z. Wang, J. Qiu, Y. Zhou, Y. Shi, L. Fu, W. Chen, and K. B. Letaief, "Federated learning via intelligent reflecting surface," *IEEE Trans. Wireless Commun.*, pp. 1–1, 2021, doi:10.1109/TWC.2021.3099505.
- [34] T. Sery, N. Shlezinger, K. Cohen, and Y. C. Eldar, "Over-the-air federated learning from heterogeneous data," *IEEE Trans. Signal Process.*, vol. 69, pp. 3796–3811, Jun. 2021.
- [35] R. Paul, Y. Friedman, and K. Cohen, "Accelerated gradient descent learning over multiple access fading channels," *IEEE J. Sel. Areas Commun.*, pp. 1–1, 2021, doi:10.1109/JSAC.2021.3118410.
- [36] S. Liu, P.-Y. Chen, B. Kailkhura, G. Zhang, A. O. Hero III, and P. K. Varshney, "A primer on zeroth-order optimization in signal processing and machine learning: Principals, recent advances, and applications," *IEEE Signal Process. Mag.*, vol. 37, no. 5, pp. 43–54, Sept. 2020.
- [37] A. Nemirovski, A. Juditsky, G. Lan, and A. Shapiro, "Robust stochastic approximation approach to stochastic programming," *SIAM J. Optim.*, vol. 19, no. 4, pp. 1574–1609, 2009.
- [38] Y. Nesterov and V. Spokoiny, "Random gradient-free minimization of convex functions," *Foundations of Computational Mathematics*, vol. 17, no. 2, pp. 527–566, 2017.
- [39] S. Ghadimi and G. Lan, "Stochastic first- and zeroth-order methods for nonconvex stochastic programming," *SIAM J. Optim.*, vol. 23, no. 4, pp. 2341–2368, 2013.
- [40] J. C. Duchi, M. I. Jordan, M. J. Wainwright, and A. Wibisono, "Optimal rates for zero-order convex optimization: The power of two function evaluations," *IEEE Trans. Inf. Theory*, vol. 61, no. 5, pp. 2788–2806, May 2015.
- [41] O. Abari, H. Rahul, D. Katabi, and M. Pant, "Airshare: Distributed coherent transmission made seamless," in *Proc. IEEE Conf. Comput. Commun. (INFOCOM)*, 2015, pp. 1742–1750.
- [42] A. Mahmood, M. I. Ashraf, M. Gidlund, J. Torsner, and J. Sachs, "Time synchronization in 5G wireless edge: Requirements and solutions for critical-mtc," *IEEE Commun. Mag.*, vol. 57, no. 12, pp. 45–51, 2019.
- [43] N. Carlini and D. Wagner, "Towards evaluating the robustness of neural networks," in *Proc. Symp. Security Privacy (SP)*, 2017.
- [44] X. Gao, B. Jiang, and S. Zhang, "On the information-adaptive variants of the ADMM: An iteration complexity perspective," *J. Sci. Comput.*, vol. 76, no. 1, pp. 327–363, 2018.